NAA-SR-3096

COPY

MASTER

EXPONENTIAL EXPERIMENTS WITH GRAPHITE LATTICES CONTAINING MULTIROD SLIGHTLY ENRICHED URANIUM FUEL CLUSTERS

AEC Research and Development Report

ATOMICS INTERNATIONAL

A DIVISION OF NORTH AMERICAN AVIATION, INC.

NAA-SR-3096
PHYSICS AND MATHEMATICS
46 PAGES

EXPONENTIAL EXPERIMENTS WITH GRAPHITE LATTICES CONTAINING MULTIROD SLIGHTLY ENRICHED URANIUM FUEL CLUSTERS

BY

W. W. BROWN
F. L. FILLMORE
B. L. SCOTT

ATOMICS INTERNATIONAL

A DIVISION OF NORTH AMERICAN AVIATION, INC.
P.O. BOX 309 CANOGA PARK, CALIFORNIA

CONTRACT: AT(11-1)-GEN-8
ISSUED: JANUARY 15, 1959

DISTRIBUTION

This report has been distributed according to the category "Physics and Mathematics" as given in "Standard Distribution Lists of Unclassified Scientific and Technical Reports" TID-4500 (14th Ed.), October 1, 1958. A total of 650 copies was printed.

CONTENTS

FIGURES

FIGURES (Continued)

TABLES

ABSTRACT

Studies of 13 exponential experiments with graphite moderated lattices containing multirod fuel clusters are presented. The bucklings and detailed intracell flux distributions were measured for each lattice. Average flux values for each material of the unit cell are given. The theoretical analysis yields a value of the effective resonance integral and of the resonance neutron inverse diffusion length in the moderator, which can be used in 2-group sodium graphite reactor calculations. The results are:

1) $\mathscr{L}_m = 0$. This implies no excess absorption, or $E - 1 = 0$.

2) $$\begin{cases} \left(\int \sigma_{res}\right)_{eff} = \dfrac{7.0}{F} + 29.5\,\dfrac{S}{M}\ barns \\ \left(\int \sigma_{res}\right)_{eff} = 2.0 + 24.7\sqrt{\dfrac{S}{M}}\ barns \quad . \end{cases}$$

There is evidence that neutron spectral hardening corrections are important, but a crude treatment of this effect did not improve the fit to the experimental measurements. The calculations are presented in detail, and various lattice parameters are tabulated.

I. INTRODUCTION

For several years, Atomics International has been developing the sodium graphite reactor concept. As a part of this program, the Sodium Reactor Experiment, designated by SRE, was undertaken. Along with the SRE program, it was decided to conduct a series of exponential experiments using graphite moderator and slightly enriched uranium fuel. The purpose of these experiments was to provide information necessary for improving the reliability of neutron calculations for sodium graphite reactors.

One of the most perplexing aspects of these calculations for the reactor types being considered was the fuel element geometry. In order to improve the removal of heat from the fuel, it was proposed to use fuel elements which comprised clusters of uranium rods instead of a single large rod. The effect of this proposed fuel geometry on reactor calculations was not known. Since a careful theoretical evaluation of this effect was difficult, it was decided that some experiments using this type of fuel geometry were needed in order to support the calculations. One of the fuel clusters used in these experiments was to represent as closely as practical the cluster chosen for the SRE. The difficulties associated with handling sodium make it unattractive for use in exponential experiments, so it was decided to mock up the sodium in the fuel element by aluminum. The macroscopic thermal neutron properties of these two materials are nearly the same. Moreover, aluminum is a very convenient metal with which to work. Four other fuel clusters were also used. Their construction was dictated by the fuel which was readily available to us. Measurements were made on a total of 13 different lattices.

The experimental measurements consisted of determining the flux distribution for each lattice in both the horizontal and vertical directions. The material buckling for each lattice was obtained from an analysis of these results. In addition, very detailed measurements were made of the flux distribution within a lattice cell; and the average flux in each material of the cell was calculated. These results are herewith presented, together with graphs of typical intracell flux distributions.

The goal of the theoretical analysis was not only to correlate the experimental results, but also to improve the reliability of the well known 2-group method for

calculations on lattices of this kind. The emphasis was on simplicity, rather than close accuracy, although reasonably accurate and reliable results were desired. The 2-group treatment being basically semiempirical, it was hoped that the stated ends could be achieved by allowing one or more of the quantities involved in the calculations to be parameters. The value of any such parameter was then to be taken from analysis of the exponential experiments. It was decided to follow, with a few variations, the method introduced by P. W. Mummery[1] for this analysis. However, the effective resonance integral was chosen as the sole parameter to be adjusted, instead of including also eta as a parameter, as Mummery had done. This decision was made when it became apparent that our data did not yield the well defined straight lines expected from this method of analysis. A consequent uncertainty of several percent would have been introduced into an experimental determination of eta. It was, therefore, decided to calculate eta and attempt to fit the experimental results by treating only the effective resonance integral as a parameter.

The analysis was made using both the age diffusion and the 2-group criticality conditions. As might be expected, the age diffusion yields a better fit to the experimental results than does the latter condition. However, for use in 2-group reactor calculations, the parameter should be obtained by means of the 2-group equation.

II. EXPERIMENTAL MEASUREMENTS

A. THE EXPONENTIAL ASSEMBLIES

A sketch of the apparatus used for the experiments is shown in Figure 1. A water boiler reactor was used as the source of neutrons for the measurements, and the exponential experiment assembly was placed on the top surface of the graphite reflector of the reactor. This assembly consisted of 7-inch square graphite stringers, each 64 inches high. There was a 2.90-inch diameter hole along the axis of each stringer for insertion of the fuel elements. Thirty-six of these stringers were used to form a 6 by 6 array of lattice cells with a 7-inch square lattice spacing. Graphite spacer blocks were provided so that lattices with a 9-1/2-inch and a 12-inch spacing could also be constructed. A top view of an assembly with a 12-inch lattice spacing is shown in Figure 2. The eyebolt at the center of the picture is used to remove the vertical foil holder on the axis of the assembly. The top portion of each hole provided for the fuel elements was threaded, permitting insertion of a lifting tool for handling the large graphite blocks with the overhead crane. A cadmium sheet covered the four sides of the assembly to prevent entry of thermal neutrons through these sides.

Fuel holders for the exponential experiments were constructed of aluminum cylinders 2.872 inches in outside diameter. Holes were drilled parallel to the axis of the cylinders for insertion of uranium slugs. Since the aluminum cylinders were made in 6-inch lengths, additional holes were provided for tie rods to hold 10 cylinders together so as to form a completed fuel element. As shown on the right side of Figure 1, two types of fuel holders were available for the experiments. One type had provision for seven fuel rods, each 3/4 inch in diameter; and the other type had provision for four fuel rods, each 1 inch in diameter. An end view of a 7-rod fuel element is shown in Figure 3. The wooden support seen in the photograph aided in handling the fuel element when fuel slugs were inserted. A 6-rod element could be formed from a 7-rod element by removal of the central rod. Lattices were studied in which this central fuel rod was replaced either by an aluminum or a graphite rod. Pertinent details defining the geometries of these lattices and the materials used in them are given in Tables I and II, and in Figure 4.

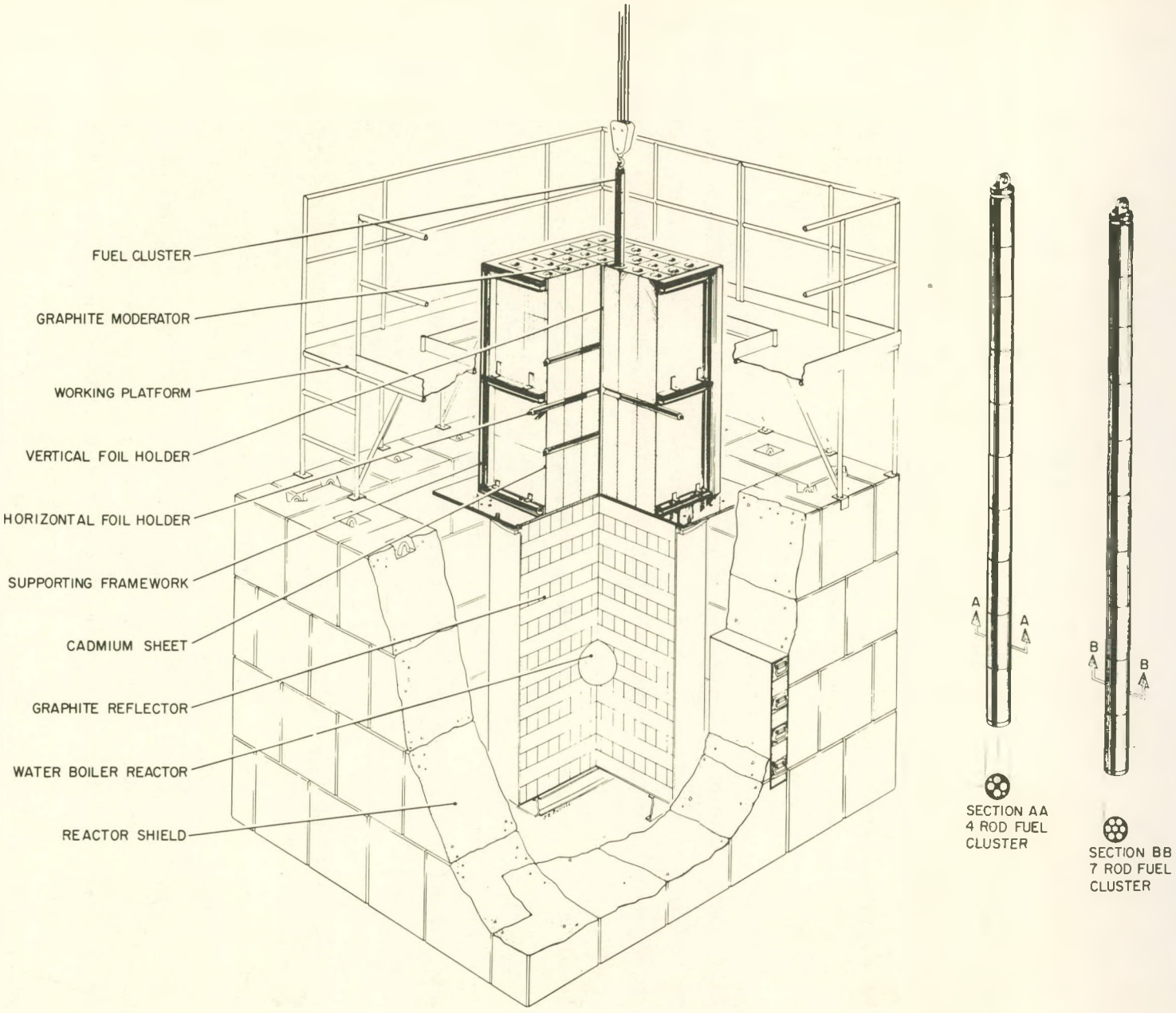

Figure 1. Cutaway View of Exponential Assembly and Water Boiler Reactor

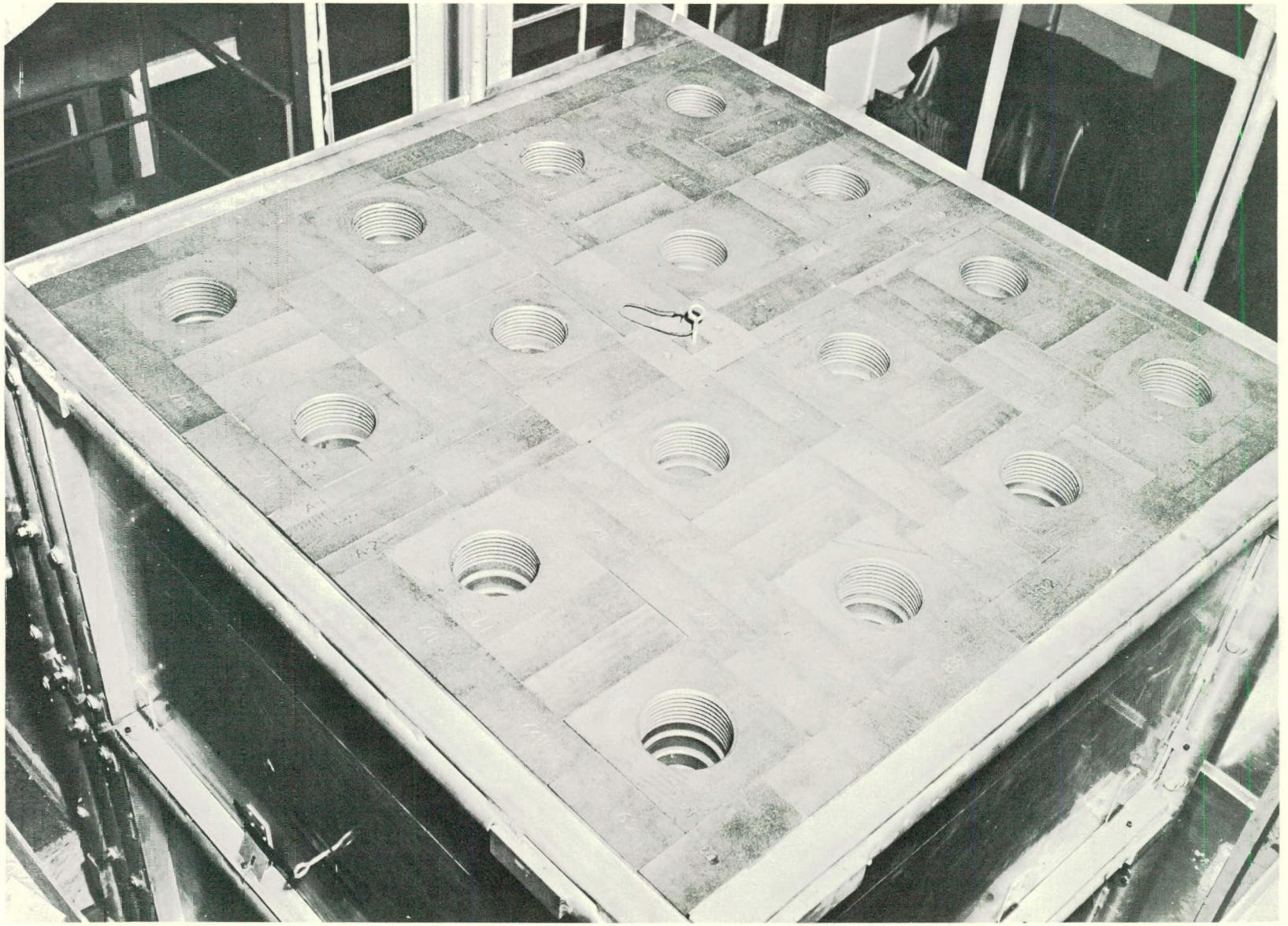

Figure 2. Top View of Exponential Assembly with 12-in. Lattice Spacing

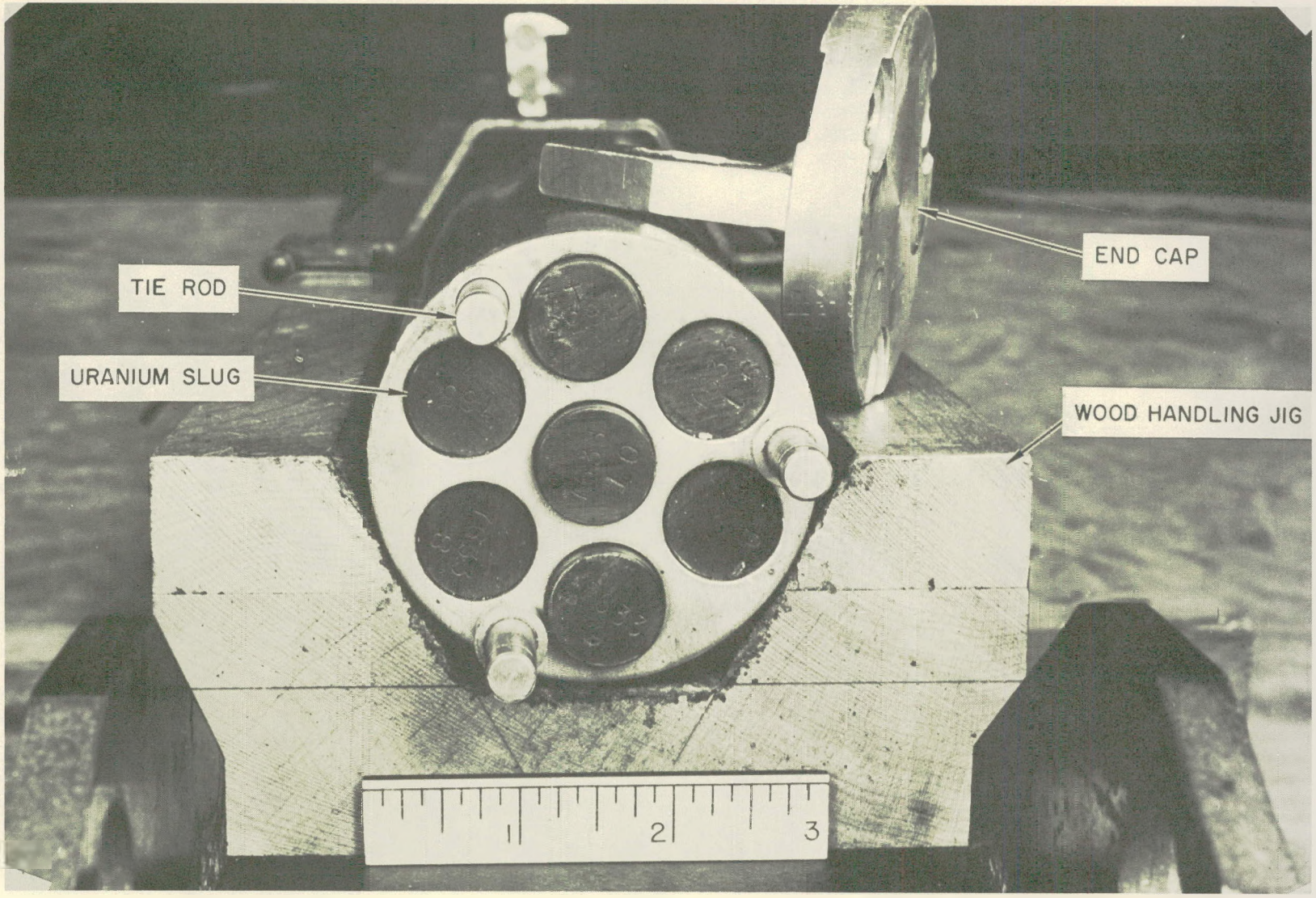

Figure 3. End View of 7-Rod Fuel Element

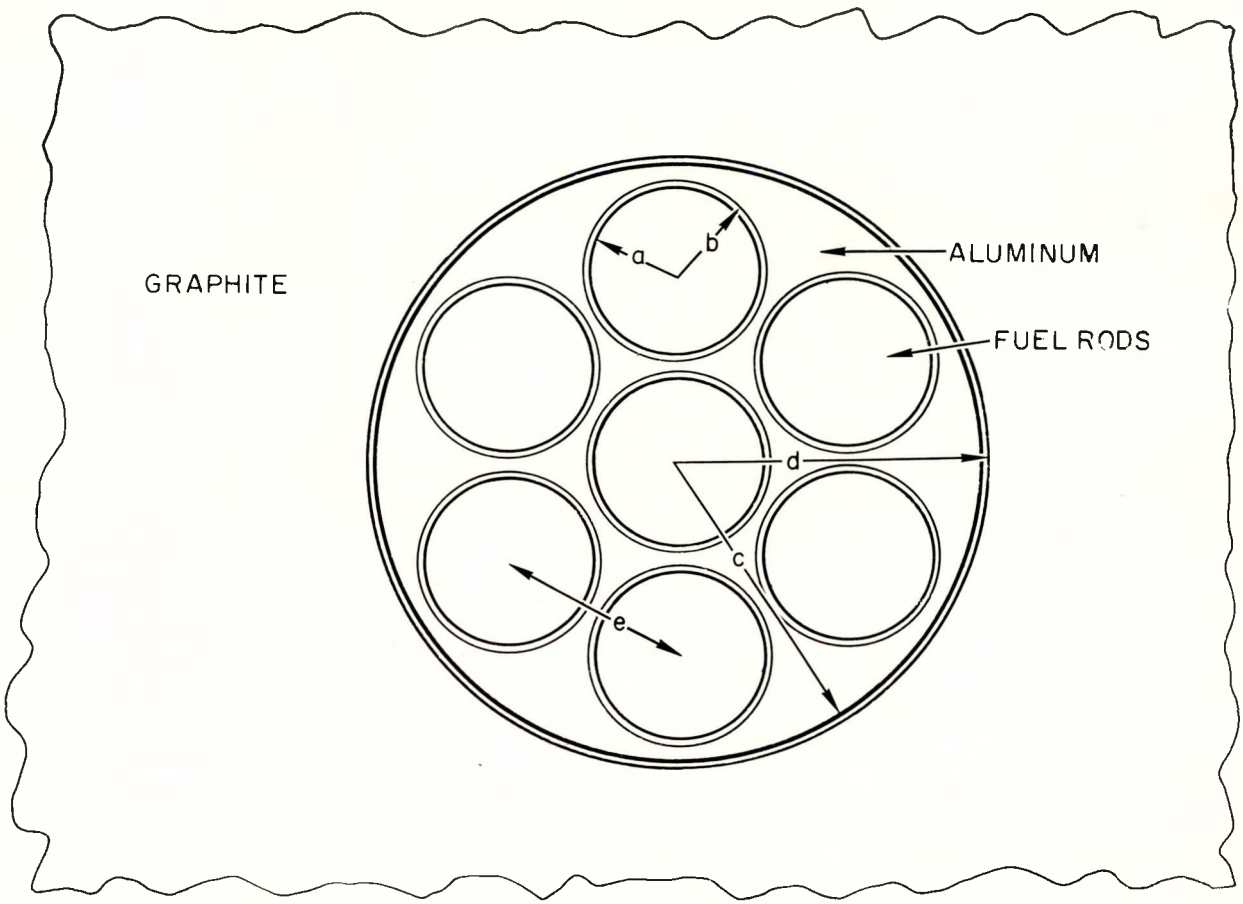

Figure 4. Definitions of Dimensions Used to Describe Cell and Fuel Element Geometry

TABLE I

CELL DIMENSIONS FOR THE EXPONENTIAL LATTICES

Lattice Spacing (in.)	Fuel*	No. of Fuel Rods	ℓ† (in.)	a (in.)	b (in.)	c (in.)	d (in.)	e (in.)	No. of Unit Cells
7.0	SRE§	7	7.002	0.376	0.3795	1.436	1.450	0.905	36 (6 x 6)
9.5	SRE	7	9.501	0.376	0.3795	1.436	1.450	0.905	25 (5 x 5)
12.0	SRE	7	12.005	0.376	0.3795	1.436	1.450	0.905	16 (4 x 4)
7.0	SRE	6 center rod of carbon	7.002	0.376	0.3795	1.436	1.450	0.905	36 (6 x 6)
9.5	SRE	6 center rod of carbon	9.501	0.376	0.3795	1.436	1.450	0.905	25 (5 x 5)
12.0	SRE	6 center rod of carbon	12.005	0.376	0.3795	1.436	1.450	0.905	16 (4 x 4)
7.0	SRE	6 center rod of aluminum	7.002	0.376	0.3795	1.436	1.450	0.905	36 (6 x 6)
7.0	0.901 wt%	4	7.002	0.498	0.504	1.436	1.450	1.281	36 (6 x 6)
9.5	0.901 wt%	4	9.508	0.498	0.504	1.436	1.450	1.281	36 (6 x 6)
12.0	0.901 wt%	4	12.005	0.498	0.504	1.436	1.450	1.281	16 (4 x 4)
7.0	natural	7	7.002	0.3735	0.3795	1.436	1.450	0.905	36 (6 x 6)
9.5	natural	7	9.508	0.3735	0.3795	1.436	1.450	0.905	36 (6 x 6)
12.0	natural	7	12.005	0.3735	0.3795	1.436	1.450	0.905	16 (4 x 4)

*The densities of the natural, SRE, and 0.901 percent (by wt) enriched fuels used were 18.88, 18.88 18.83 gm/cm^3 respectively.

† The literal dimensions are defined in Figure 4.

§"SRE" indicates the 2.778 percent (by wt) enriched fuel subsequently used in the Sodium Reactor Experiment.

TABLE II

MATERIAL DENSITIES FOR THE EXPONENTIAL LATTICES

Lattice Spacing (in.)	Graphite Density (gm/cm^3)	Aluminum Density (gm/cm^3)
7.0	1.711	2.668
9.5	1.733	2.668
12.0	1.719	2.668
9.5 (with SRE fuel)	1.714	2.668

Aluminum was chosen for construction of the fuel holders, not only because it provided an adequate mockup for the sodium used in the proposed reactor system, but also because aluminum is easily obtained, readily machined, and has no long-lived radioactive products. The macroscopic absorption and scattering cross sections of the aluminum used are 0.0121 cm^{-1} and 0.0834 cm^{-1} respectively, corresponding to values for sodium of 0.013 cm^{-1} and 0.089 cm^{-1}.

B. MEASUREMENTS IN GRAPHITE

Since the thermal diffusion length in graphite is strongly dependent on the purity of the graphite used, this length was measured for each lattice assembly. This operation was done by first plugging the fuel element channels with 2.9 inch diameter graphite cylinders, to make a solid graphite stack. The thermal neutron distributions along vertical and horizontal directions were then measured by foil activation techniques. These distributions are given respectively by $\sinh \nu(z - h)$ and $\cos \mu x \cos \mu y$, where z is the height above the bottom of the stack of height h, and where x and y are horizontal rectangular coordinates measured from the vertical axis of the stack. Horizontal distributions were measured at three levels, namely, at 18, 30, and 42 inches above the bottom of the stack.

In some instances, because of the geometric mismatch of the square graphite stack to the cylindrical graphite thermal column, the presence of a third harmonic contribution to the horizontal distribution was detected. From the data, a measure of the amplitude of the harmonic and an estimate of its attenuation could

be made. Wherever necessary, the vertical distribution data were corrected to remove the contribution of the third harmonic along the vertical axis. The amplitude of the third harmonic was in all cases less than 2 percent of the first harmonic.

Analysis of the corrected data gave values of μ and ν for each assembly. The thermal neutron diffusion lengths are given by the relation $L^{-2} = \nu^2 - 2\mu^2$. Table III shows the results for each of the graphite assemblies. The graphite densities given differ slightly from those quoted in Table II because of small changes during restacking. The four measurements agree with one another, and have the average value, $L = 50.5\,cm \pm 0.8\,cm$. With the graphite plugs in place, the average graphite density was 1.713 gm/cm^3. The values of μ define the effective lateral dimensions of each assembly. The extrapolated width in each case is given by π/μ.

TABLE III

THERMAL NEUTRON DIFFUSION LENGTH
FOR AGOT GRAPHITE ASSEMBLIES

Actual Width of Assembly (in.)	Graphite Density (gm/cm^{-3})	μ (m^{-1})	ν (m^{-1})	Diffusion Length, (cm)
42	1.704	2.833	4.469	51.3
47.5	1.729	2.512	4.067	50.8
48	1.707	2.486	4.034	50.9
57	1.7114	2.111	3.617	49.1

C. BUCKLING MEASUREMENTS

The measurements of lattice buckling were made by using a procedure similar to that used for the diffusion length measurements; except that, necessarily, the effective dimensions of the assembly in the horizontal plane were taken directly from the results of the measurements in the pure graphite. Values of ν were determined from the measured thermal flux distributions along the vertical axis

of the lattices. The bucklings are $B^2 = 2\mu^2 - \nu^2$, and the results for each of the lattices investigated are listed in Table IV. The results are also shown graphically in Figure 5.

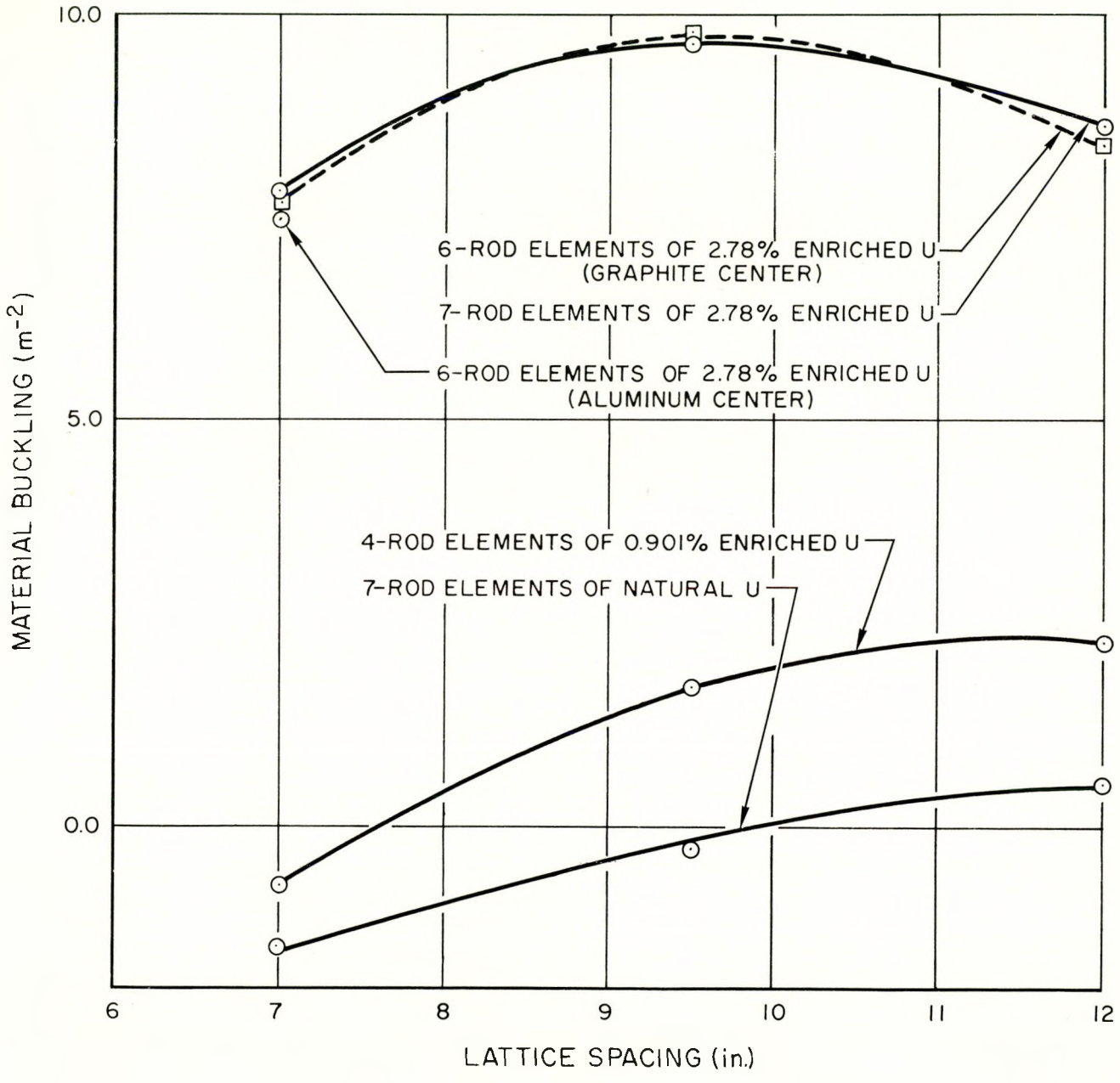

Figure 5. Lattice Bucklings Measured in the Exponential Experiment

TABLE IV

MEASURED LATTICE BUCKLINGS AND AVERAGE THERMAL NEUTRON FLUXES IN THE FUEL AND ALUMINUM

Lattice Spacing (in.)	Fuel	Buckling (m^{-2})	Average Thermal Neutron Flux§		
			Central Rod	Outer Rod	Aluminum
7.0	7-rod Natural	-1.50 ± 0.15	0.378	0.478	0.584
9.5	7-rod Natural	-0.35 ± 0.15	0.317	0.407	0.512
12.0	7-rod Natural	0.53 ± 0.15	0.287	0.367	0.466
7.0	7-rod SRE	7.81 ± 0.21	0.170	0.281	0.453
9.5	7-rod SRE	9.67 ± 0.17	0.127	0.223	0.371
12.0	7-rod SRE	8.64 ± 0.09	0.104	0.190	0.329
7.0	6-rod SRE*	7.69 ± 0.35	-	0.303	0.465
9.5	6-rod SRE*	9.76 ± 0.18	-	0.238	0.392
12.0	6-rod SRE*	8.37 ± 0.35	-	0.201	0.336
7.0	6-rod SRE†	7.49 ± 0.40	-	0.310	0.448
7.0	4-rod 0.901%	-0.77 ± 0.64	-	0.427	0.567
9.5	4-rod 0.901%	1.67 ± 0.28	-	0.355	0.495
12.0	4-rod 0.901%	2.24 ± 0.14	-	0.324	0.455

*3/4-in. graphite rod filling central channel of element.
†3/4-in. aluminum rod filling central channel of element.
§The flux values are relative to an average value of 1.000 in the graphite in each lattice, including the central rod of the element if of graphite. It is estimated that the experimental error in the flux values is about one percent.

D. INTRACELL FLUX DISTRIBUTION MEASUREMENTS

Measurements of the intracell thermal neutron flux distributions were made by activating small foils which contained dysprosium oxide. This compound was mixed with epon plastic, and the mixture then spread on a 3-mil thick aluminum backing foil, where it was allowed to harden. Foils, 2 mm by 10 mm in area, were then punched out and intercalibrated in sets by exposing a set of foils on a rotating disc to flux from the water boiler reactor. To make flux distribution

measurements, the foils were placed in grooves machined for this purpose in graphite plugs that extended horizontally through portions of the graphite. Foils could also be placed in grooves which were machined in segments of the fuel slugs.

Figure 6 shows a horizontal cross section of a typical lattice cell. The positions at which foils can be placed for flux distribution measurements are indicated. Both bare and cadmium covered foils were exposed in these locations so that the thermal neutron flux distribution could be determined throughout the cell. For

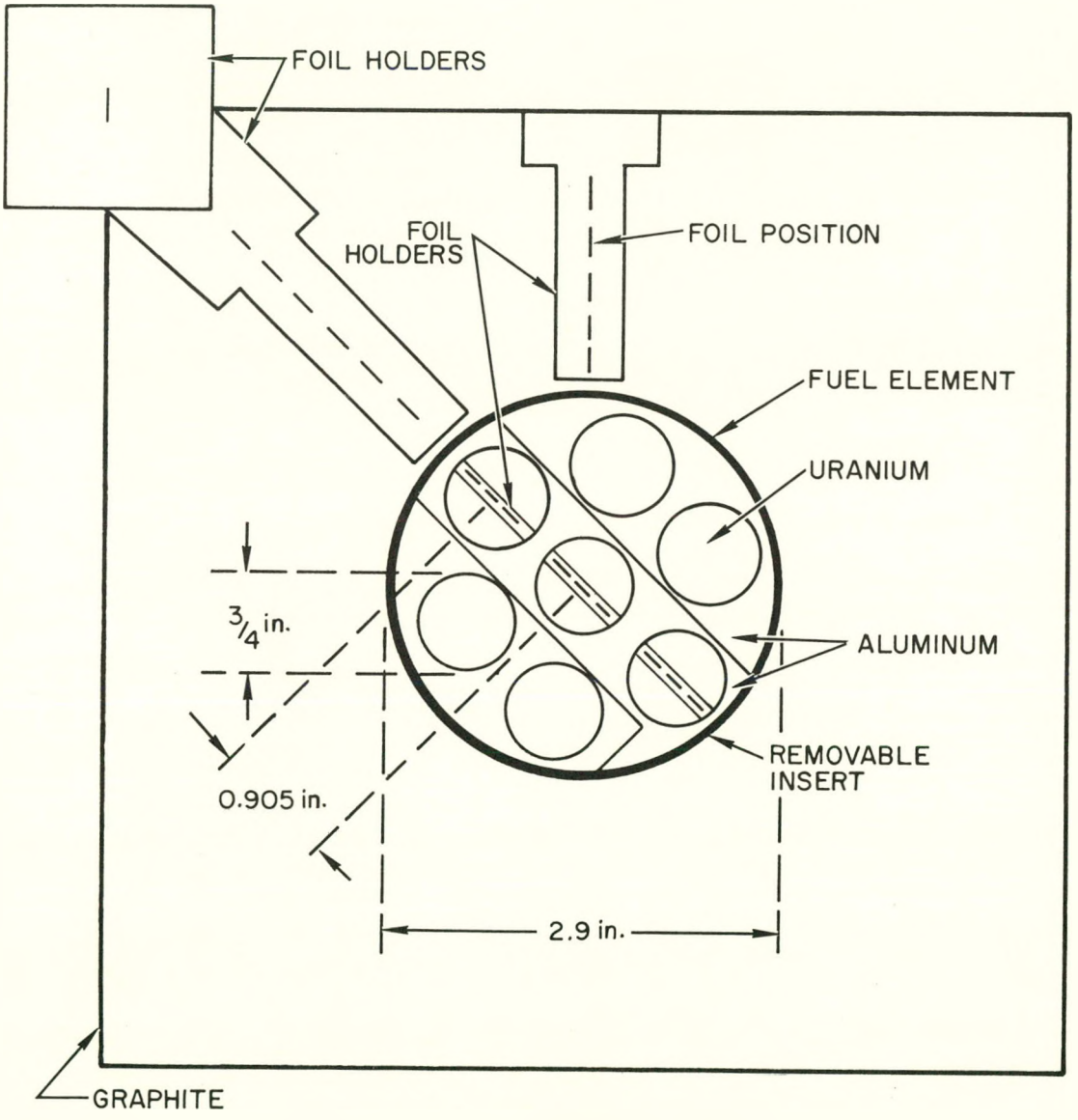

Figure 6. Horizontal Cross Section of a Typical Lattice Cell at the Level Where Detailed Flux Distributions were Measured

each lattice, the detailed flux measurements were made in a cell at or nearest the lattice center, and at a height of 18 in. above the bottom of the lattice. The observed data were divided by a factor $\cos \mu x \cos \mu y$, where x and y are the horizontal coordinates of the data point with reference to the lattice axis, and where μ^2 is the horizontal lattice buckling. This correction transforms the observed flux to that which would exist in a cell situated in a lattice of infinite extent. Figures 7 and 8 show typical flux distributions along the diagonal of a cell for some of the 6- and 7-rod element lattices.

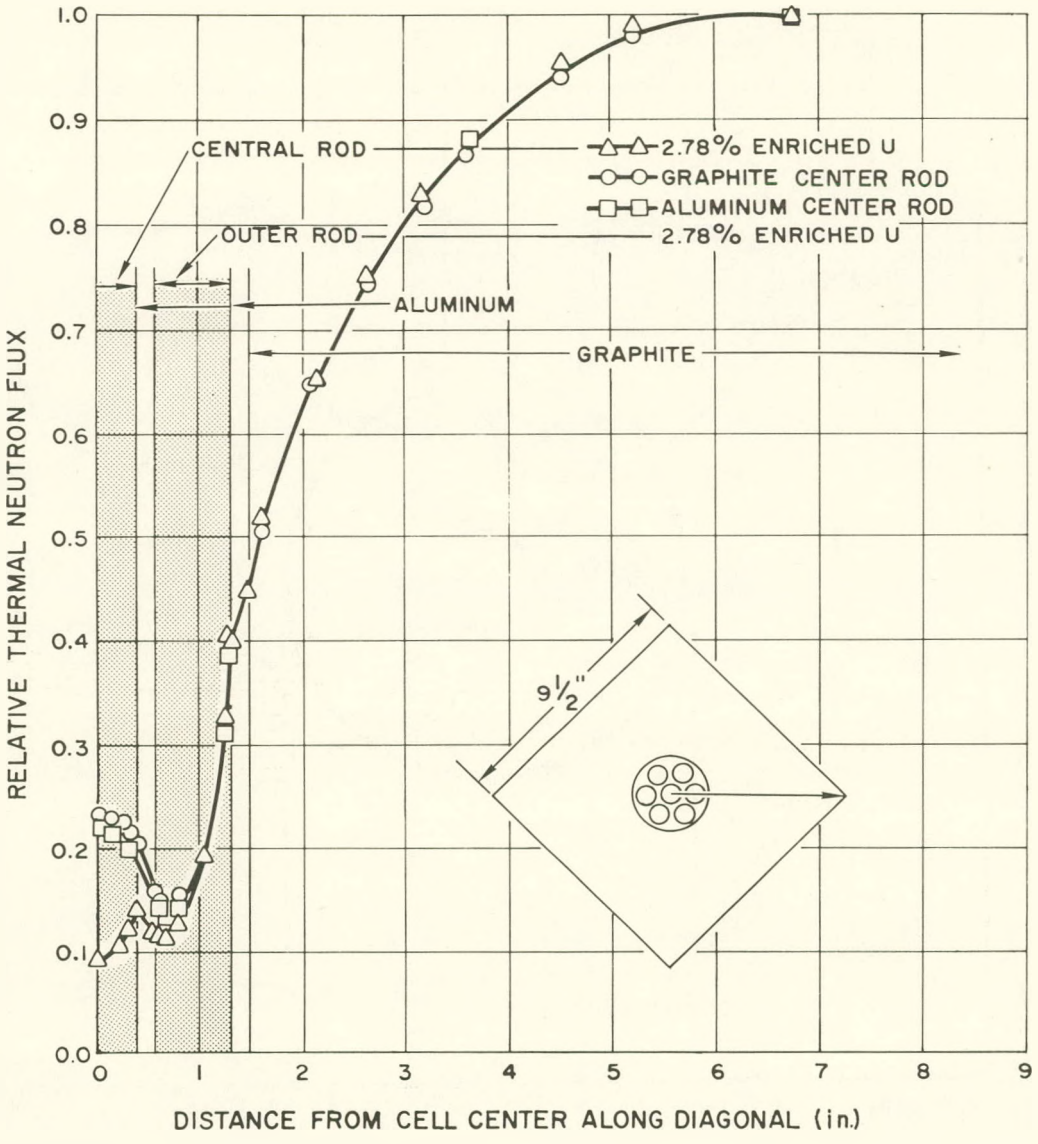

Figure 7. Typical Intracell Flux Distribution Data for 6- and 7-Rod Fuel Elements

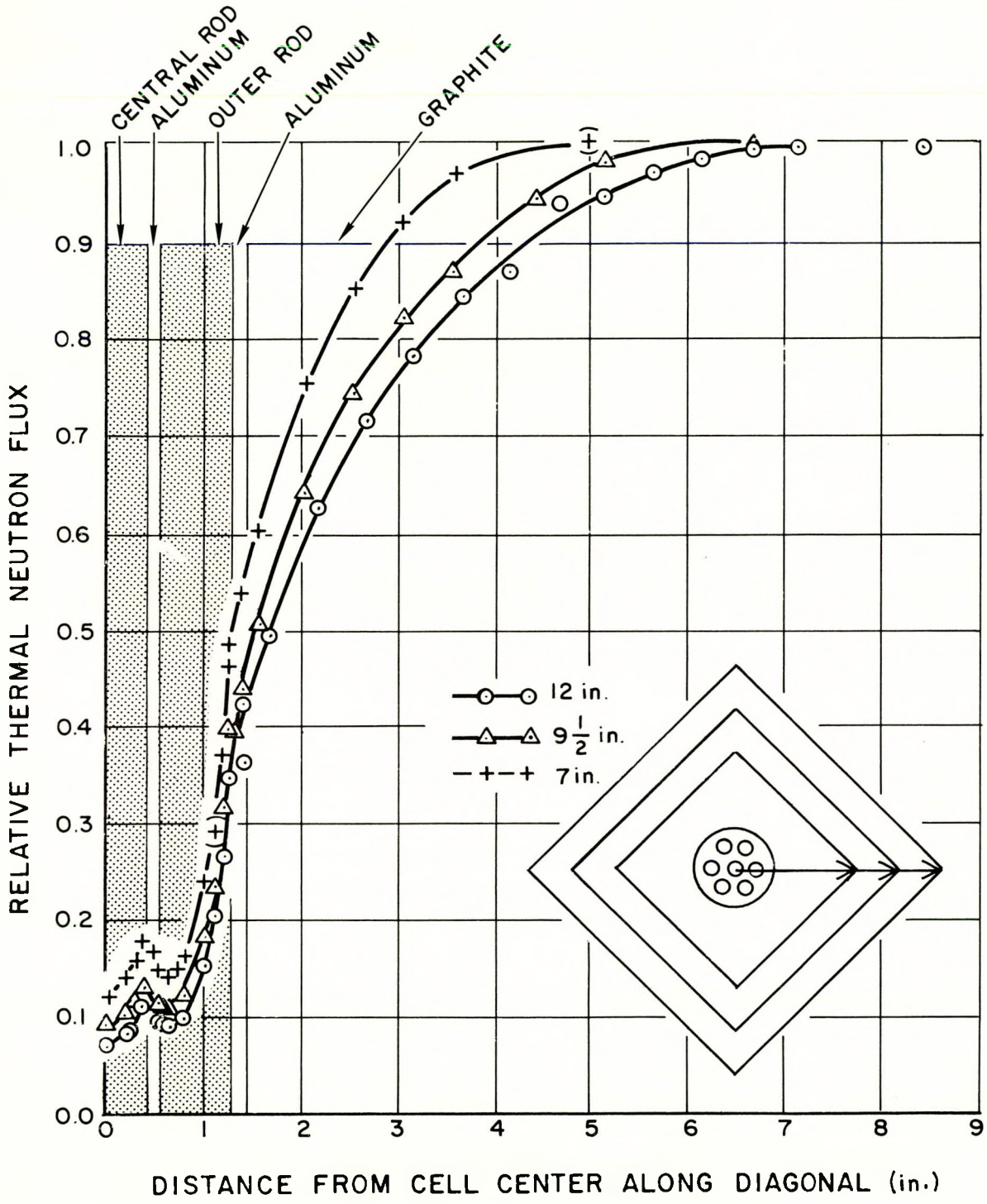

Figure 8. Intracell Flux Distributions for 6- and 7-Rod SRE Fuel Elements at Three Different Lattice Spacings

In order to obtain the average flux in each cell material, the flux must be known not only along the diagonal of the cell, but also at every other point. Flux measurements along the cell diagonal sufficed for the central fuel rod, since this distribution was symmetrical about the cell axis. In the graphite, the distributions were measured along the cell diagonal and also in a direction at 45° to this, as indicated in Figure 6. The results of these traverses showed that the distribution in the graphite was also nearly axially symmetrical. The distributions in the outer rods, however, were not axially symmetrical. A 2-dimensional survey of the flux in these rods was obtained by making diametrical flux traverses at angles of 0°, 45°, and 90° to the cell diagonal. Typical distributions of this kind are shown in Figure 9 for the outer rod of a 7-rod SRE loaded element in a 9.5-in. spaced lattice.

Data of the type shown in Figures 7, 8, and 9 were obtained for all 13 of the lattices investigated. From such data, the average thermal neutron flux in the fuel, moderator, and aluminum was determined by graphical integration. The results are summarized in Table IV, where the fluxes in the fuel and aluminum are given, relative to the flux in the graphite.

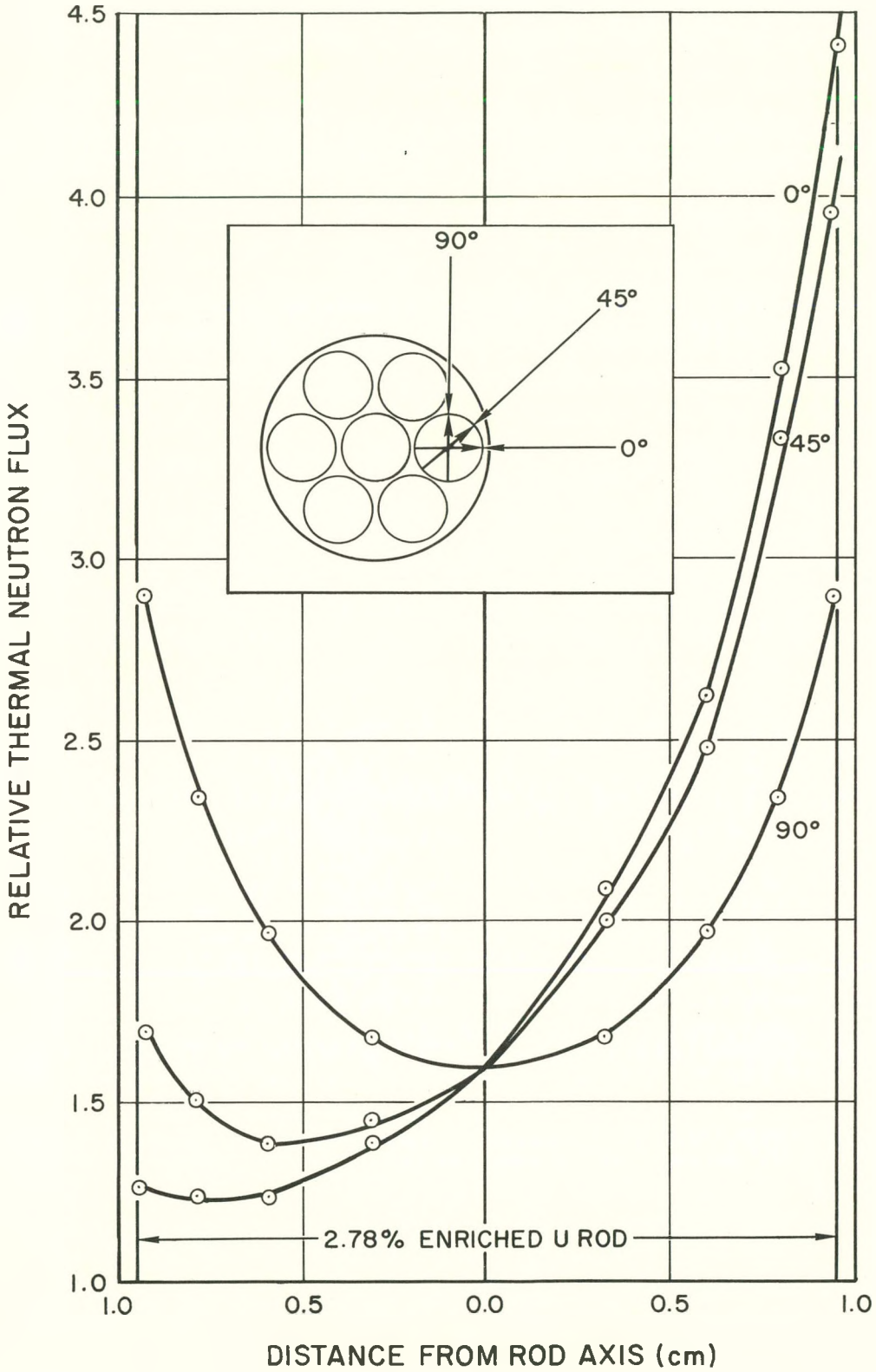

Figure 9. Flux Distribution in the Outer Rod of a 7-Rod Element

III. THEORETICAL ANALYSIS

A. EVALUATION OF THE LATTICE PARAMETERS

The 13 lattices described in Part II were analyzed not only so as to correlate the experimental results, but also so as to improve the reliability of 2-group calculations on sodium graphite reactors. A semiempirical approach was adopted in which the buckling measurements were used to determine a value for the resonance escape probability for each lattice. The effective resonance integral and $\mathcal{K}_m$, the inverse diffusion length for resonance neutrons in the moderator, were chosen as adjustable parameters with which the experimental results were to be fitted.

According to age-diffusion theory, the fundamental equation relating the lattice parameters is:

$$\frac{\eta \epsilon f p e^{-\tau B^2}}{1 + L^2 B^2} = 1 \ , \qquad \ldots(1)$$

where

η = no. of fast neutrons released per capture in fuel

ϵ = fast fission factor

f = thermal utilization

p = resonance escape probability

τ = age to thermal energy

L^2 = thermal diffusion length

B^2 = buckling.

All quantities in Equation (1) except p were calculated for each lattice by the procedures given below. Equation (1) then determines a value of p for each lattice. The quantity p was chosen to be determined by experiment, because it is believed that its theoretical calculation is less reliable than that of the other lattice parameters.

The set of values obtained for p was then used in an attempt to evaluate two parameters in a semiempirical formula for p.

The method used for the calculation of the quantities in Equation (1) will now be outlined. Most of the formulas are developed in Reference 2.

1. Eta

$$\eta = \frac{\nu \bar{\sigma}_f(25)}{\bar{\sigma}_a(25) + \dfrac{\bar{\sigma}_a(28)}{E}} \quad , \qquad \ldots(2)$$

where

ν = no. of fast neutrons per fission.

$E = N_{25}/N_{28}$ is called the atomic ratio.

The bar above the cross sections means that the cross sections are to be averaged over the thermal neutron energy distribution. It is assumed that the flux is Maxwellian, and that all cross sections vary as 1/v, with the exception of U^{235} where an f factor[3] of 0.981 has been used. Hence,

$$\bar{\sigma}_f(25) = \frac{\sqrt{\pi}}{2} (0.981)\,(580)\, b \quad .$$

2. The Fast Effect

$$(\epsilon - 1) = \frac{(\nu\sigma_f - \sigma_f - \sigma_c) P}{\sigma_t - (\nu\sigma_f + \sigma_e) P} \quad . \qquad \ldots(3)$$

The sigmas are cross sections averaged over the fission spectrum and the pertinent fuel composition. P is the first collision probability,[2] and is computed by approximating the complicated fuel cluster by a hollow cylinder. The cylinder is obtained by first replacing the outer six (or four) rods by a hollow cylinder of equal cross sectional area, so chosen that the average of its inner and outer radii is equal to the center-to-center distance of the original fuel elements. Then (for

the 7-rod clusters only) the remaining rod is spread out upon the interior of the cylinder to obtain the final figure. The results of the evaluation of P are given in Table V.

TABLE V

FIRST COLLISION PROBABILITIES

Fuel Cluster	P
7-rod SRE Fuel	0.465
6-rod SRE Fuel	0.411
4-rod Fuel Cluster	0.449
7-rod Nat. Uranium Fuel	0.461

It is assumed that η and ϵ are properties of the fuel cluster only, and thus do not depend upon the lattice dimensions. The property η should depend slightly upon the lattice spacing because of the neutron spectrum change when the fuel to moderator ratio is altered. However, it is believed that this effect is small, and it was neglected.

3. Age

$$\tau_0 = \left[\tau_f - (\tau_f - \tau_{in})\frac{\sigma_{in}}{\sigma_{tot}}P + \frac{D}{\xi\Sigma_s}\ln\frac{1.44}{5kT}\right]\left(\frac{\rho_0}{\rho}\right)^2\frac{1}{V_m} \quad . \qquad ...(4)$$

The subscript "0" on τ_0 is to prepare the notation for a future neutron streaming correction. The other symbols are defined as follows:

$\tau_f = 311 cm^2$ = age of fission neutrons to the indium resonance in graphite of density $\rho_0 = 1.60\ gm/cm^3$.

This number was obtained from Reference 4.

$\tau_{in} = 221 cm^2$ = age of inelastically scattered fission neutrons to the indium resonance in graphite of density $\rho_0 = 1.60\ gm/cm^3$.

This number was calculated by using an evaporation model for inelastically scattered neutrons, and by using Watt's fission neutron energy spectrum.

$$V_m = \sum_i V_i \frac{(\xi\Sigma_s)_i}{(\xi\Sigma_s)\,graphite} \quad .$$

V_i is the volume fraction of the i^{th} material*, and the sum is to extend over the unit cell. Thus, it is seen that V_m represents the effective volume fraction of the moderator.

$D/\xi\Sigma_s$ = 15.0 for epithermal neutrons in graphite of density 1.60 gm/cm^3.

kT = 0.0253 ev at 20°C.

The first term is the age to the indium resonance of fission spectrum neutrons in pure moderator. The second term is a correction due to inelastic scattering. The third term corrects the age to thermal energy. This was taken to be $5kT$ instead of kT, in conformity with the results obtained by E. R. Cohen.[5] Although Cohen's results were obtained for an infinite homogeneous moderator, it is believed that they are also a reasonable approximation for lattices of the type being considered.

4. Cell Averaged Cross Sections

$$\bar{\Sigma} = \frac{\sum_i \phi_i V_i \Sigma_i}{\sum_i \phi_i V_i} \quad , \qquad \ldots(5)$$

Σ_i is the macroscopic cross section for the i^{th} material. ϕ_i is the average thermal flux in the i^{th} material, which is obtained from experiment. These averaged cross sections are used to calculate the thermal diffusion length, L^2, as shown in Equation (6).

*The small voids surrounding the fuel rods and the aluminum fuel holder are assumed in this calculation to be filled with aluminum; thus, V_{al} includes V_{void}.

5. Thermal Diffusion Length

$$\frac{1}{L_0^2} = 3\overline{\Sigma}_a \overline{\Sigma}_{tr} , \qquad ...(6)$$

where

$$\overline{\Sigma}_{tr} = \overline{\Sigma}_s(1 - \overline{\mu}_0) + \overline{\Sigma}_a .$$

The subscript "0" on L_0^2 has the same significance as was stated in the equation for the age. This method of calculating a cell averaged L^2 gives a value appropriate for an equivalent homogeneous medium whose absorption and collision densities are equal to the average values of the corresponding densities for a lattice cell.

6. Thermal Utilization

$$f = \frac{\phi_{fuel} V_{fuel} \Sigma_{a\ fuel}}{\sum_i \phi_i V_i \Sigma_{a_i}} = \frac{thermal\ absorption\ in\ fuel}{total\ thermal\ absorption\ in\ cell} . \qquad ...(7)$$

7. Resonance Escape Probability

It was assumed that p is given by the following formula:

$$p = exp\left(-\frac{1}{G}\right),$$

where

$$G = \frac{V_m(\xi\Sigma_s)_{graphite}}{V_{fuel} N_{fuel} \left(\int \sigma_{res} \frac{dE}{E}\right)_{eff}} + (E - 1) . \qquad ...(8)$$

$(E - 1)$ is the "excess absorption" term for resonance neutrons. It is calculated by assuming that the square unit cell can be replaced by a circle of equal area,

$(R_1 = l\sqrt{\pi})$. Then, if d is the radius of the center hole in the graphite, it can be shown that:[2]

$$E = \frac{(R_1^2 - d^2)}{2d} \mathscr{K}_m \frac{I_0(\mathscr{K}_m d) K_1(\mathscr{K}_m R_1) + K_0(\mathscr{K}_m d) I_1(\mathscr{K}_m R_1)}{I_1(\mathscr{K}_m R_1) K_1(\mathscr{K}_m d) - K_1(\mathscr{K}_m R_1) I_1(\mathscr{K}_m d)} .$$

where I and K represent modified Bessel Functions of the first and second kinds, and where $\mathscr{K}_m$ is the inverse diffusion length for resonance neutrons in graphite. The two parameters, $\mathscr{K}_m$ and the effective resonance integral, that appear in Equation (8) were evaluated by means of the experimental data obtained from the exponential experiments.

A formula for the effective resonance integral is chosen as a matter of convenience for making comparisons with other experimental work. No attempt is made to investigate the form of this formula because the value of the surface-to-mass ratio for all of the fuel clusters being considered covers a very narrow range. The effective resonance integral can be represented by either of the following expressions:

$$\left(\int \sigma_{res} \frac{dE}{E}\right)_{eff} = \begin{cases} \dfrac{A}{F} + 29.5\dfrac{S}{M} \\ A' + 24.7\sqrt{\dfrac{S}{M}} \end{cases} . \qquad \ldots(9)$$

The value of the coefficient of the S/M term is taken from Reference.[6] Values for A and A' were determined from analysis of the results of the exponential experiments. Most of the analyses being described were made by using the first formula. F is the disadvantage factor for resonance neutrons in the fuel. We assume in calculating F that all of the fuel rods have been combined to form one large cylinder with the original total cross sectional area. If this cylinder has a radius R, then

$$F = \frac{\mathscr{K}_u R}{2} \frac{I_0(\mathscr{K}_u R)}{I_1(\mathscr{K}_u R)} ,$$

where

$$\mathcal{K}_u = 0.42\,cm^{-1} \quad .$$

S/M is the surface to mass ratio per unit length of the fuel cluster, and is computed by using the surface which would be determined by encircling the cluster with a tight rubber band. This is a valid approximation because most of the fuel clusters will not allow a neutron to pass through without making a collision in the fuel. Also, the mean free path of neutrons in the aluminum is large compared to the dimensions of the gaps between fuel rods, so that the probability of a neutron being scattered out of the fuel cluster is small. For the 4-rod and 6-rod clusters, an appropriate amount of the surface was deleted to take into account the ability of a neutron to pass directly through these clusters.

In the aforementioned equations, there has been no mention of the inevitable voids which are present and which should be considered in the calculation. These voids (surrounding each fuel rod and the entire cluster) permit neutron streaming which affects the age and thermal diffusion lengths. A correction for this streaming was made according to the method developed by Behrens,[7] and is represented by Equation (10).

$$\left(\frac{\Lambda}{\Lambda_0}\right)^2 = 1 + 2H + \frac{H^2\left(\frac{2r}{H\lambda}\right)}{exp\left(\frac{2r}{H\lambda}\right) - 1} + \frac{rHQ}{\lambda} \quad . \qquad \ldots(10)$$

H is the ratio of the volume of the void to that of the material, and is shown in Table VI together with the correction factor. Calculation shows the last two terms to be of the order of 0.01 percent for these lattices, so these terms were neglected. The values of τ and L^2, corrected for streaming, are then given by:

$$\tau = \tau_0 \left(\frac{\Lambda}{\Lambda_0}\right)^2$$

$$L^2 = L_0^2 \left(\frac{\Lambda}{\Lambda_0}\right)^2$$

It is seen from the table that the streaming corrections are small.

TABLE VI

NEUTRON STREAMING CORRECTIONS

Lattice Types	Lattice Spacing (in.)	H	$\left(\frac{\Lambda}{\Lambda_0}\right)^2$
SRE	7.0	0.00449	1.0090
	9.5	0.00243	1.0049
	12.0	0.00152	1.0030
4-rod	7.0	0.00413	1.0083
	9.5	0.00223	1.0045
	12.0	0.00140	1.0028
Natural	7.0	0.00463	1.0093
	9.5	0.00251	1.0050
	12.0	0.00157	1.0031

The absorption cross section of the graphite was calculated from the experimentally determined value of the diffusion length in the solid graphite lattice. The diffusion length was found to be $L^2 = 2555\ cm^2$ for graphite of density 1.713 gm/cm^3. This leads to $\sigma_a = 4.397 \times 10^{-3}$ barns at 2200 m/s, upon application of Equation (6). All other cross sections were obtained from BNL-325. The values used in this study are given in Tables VII and VIII.

TABLE VII

MICROSCOPIC NUCLEAR DATA

Material	σ_a(2200 m/sec) (barns)	σ_s (barns)	σ_f(2200 m/sec) (barns)	ξ*	$\bar{\mu}_0$†
U^{235}	687	10.0	580.0	0.008483	0.002800
U^{238}	2.75	8.3	0.0	0.008376	0.002836
C	0.004397	4.8	0.0	0.1578	0.05551
Al	0.230	1.4	0.0	0.07237	0.02472

$\nu_{25} = 2.47$

* ξ is the average logarithmic energy decrement per collision, and is calculated from

$$\xi = 1 + \frac{(A-1)^2}{2A} \ln \frac{A-1}{A+1} \approx \frac{2}{A + \frac{2}{3}}$$

† $\bar{\mu}_0$ is the average cosine of the scattering angle in the lab system, and is given by $\bar{\mu}_0 = 2/3A$.

TABLE VIII

CROSS SECTIONS AVERAGED OVER THE FISSION SPECTRUM

Cross Section (barns)	U^{238} (barns)	U^{235} (barns)
σ_t	7.10	7.1
σ_f	0.28	1.2
σ_{in}	1.85	1.5
σ_c	0.09	0.2
σ_e	4.88	4.2
ν	2.50	3.0
$\nu\sigma_f$	0.70	4.8

Fuel designated as SRE fuel was 2.778 w/o U^{235}; the 4-rod fuel was 0.901 w/o U^{235}, and the natural uranium was assumed to be 0.714 atomic percent U^{235}. These values lead to $E(SRE) = 0.02894$; $E(4\text{-}rod) = 0.009207$; $E(Natural) = 0.007191$ (where $E = N_{25}/N_{28}$).

The results of the above calculations for each of the lattices being studied are shown in Table IX.

TABLE IX

CALCULATED LATTICE PARAMETERS

Fuel	Lattice Spacing (in.)	η	ϵ	f	$\overline{L^2}$ (cm^2)	τ (cm^2)	p calculated from Eq (1)
7-rod SRE	7.0	1.8276	1.0434	0.9575	48.32	340.86	0.7416
	9.5	1.8276	1.0434	0.9310	112.81	310.00	0.8428
	12.0	1.8276	1.0434	0.8935	209.72	305.79	0.9031
6-rod SRE C-center	7.0	1.8276	1.0359	0.9557	49.64	338.61	0.7445
	9.5	1.8276	1.0359	0.9278	116.07	309.52	0.8572
	12.0	1.8276	1.0359	0.8896	216.48	306.11	0.9062
6-rod SRE Al-center	7.0	1.8276	1.0359	0.9549	48.40	341.80	0.7405
4-rod	7.0	1.4449	1.0351	0.9290	73.85	340.72	0.6969
	9.5	1.4449	1.0351	0.8943	160.76	316.92	0.8093
	12.0	1.4449	1.0351	0.8527	268.01	306.09	0.8903
7-rod Natural	7.0	1.3303	1.0359	0.9201	81.01	340.98	0.7401
	9.5	1.3303	1.0359	0.8848	171.72	316.94	0.8063
	12.0	1.3303	1.0359	0.8400	294.96	306.01	0.8915

B. ANALYSIS OF RESULTS

The preceding calculations have resulted in a value of p for each lattice. The next step was to see if these values could be consistently correlated. For this purpose, the semi-empirical expression for p given by Equation (8) was chosen.

This expression contains A and $\mathscr{K}_m$ as parameters to be determined by using the values of p obtained above. A method of analysis originally introduced by P. W. Mummery[1] was used. If one takes the natural logarithm of both sides of Equation (1) and makes use of Equation (8), he obtains:

$$ln(\eta\epsilon) - \frac{1}{G} = \tau B^2 + ln\left(\frac{1 + L^2B^2}{f}\right) \qquad ...(11)$$

If one assumes $\mathscr{K}_m = 0$, then $(E - 1) = 0$,

$$\frac{1}{G} = \frac{V_{fuel}N_{fuel}\left(\int \sigma_{res}\frac{dE}{E}\right)_{eff}}{V_m(\xi\Sigma_s)_{graphite}} ,$$

and (11) becomes

$$ln(\eta\epsilon) - \frac{V_{fuel}N_{fuel}}{V_m(\xi\Sigma_s)_{graphite}}\left[\left(\int \sigma_{res}\frac{dE}{E}\right)_{eff}\right] =$$

$$\tau B^2 + ln\frac{1 + L^2B^2}{f} . \qquad ...(12)$$

One can see then that if $y = \tau B^2 + ln\frac{1 + L^2B^2}{f}$ is plotted as a function of $x = \frac{V_{fuel}N_{fuel}}{V_m(\xi\Sigma_s)_{graphite}}$, a straight line should be obtained whose slope is $-\left(\int \sigma_{res}\frac{dE}{E}\right)_{eff}$, and whose y intercept is $ln(\eta\epsilon)$. The result of such a plot is seen in Figure 10, where the error indicated is that due to the experimental buckling measurement only. The lines were drawn by eye to lie (if possible) within the error limits, and to pass through the computed value of $ln(\eta\epsilon)$. Thus, there were effectively four points determining the line.

As is evident in Figure 10, the fit of the experimental points to a straight line is only fair. In particular, the points for three of the 7-in. lattices seem to

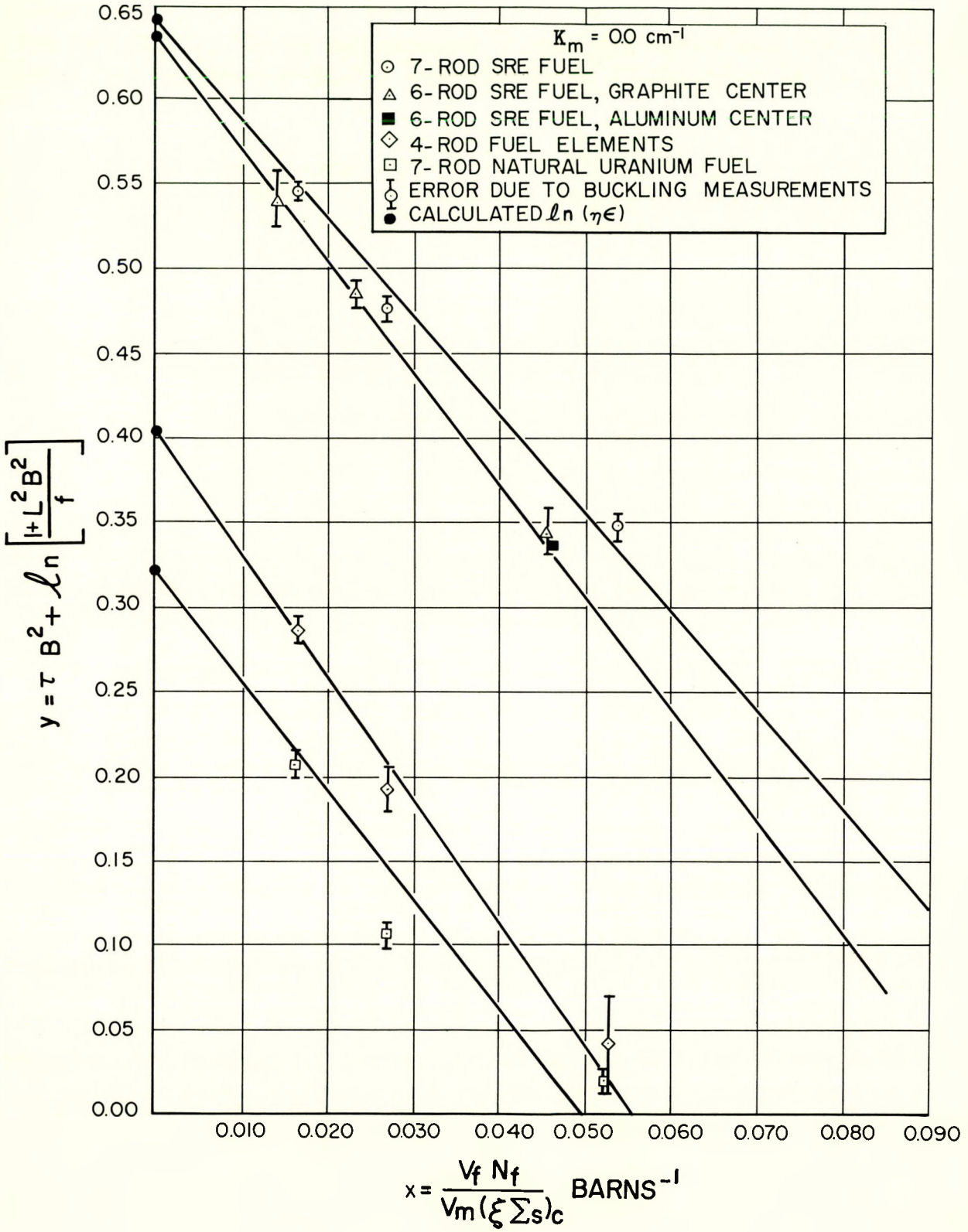

Figure 10. Plot of Equation (12)

be high. In an attempt to improve the fit, several details were investigated. First, the assumption that $\mathscr{K}_m = 0\,cm^{-1}$ was changed to $\mathscr{K}_m = 0.12\,cm^{-1}$. That is, some excess absorption was introduced. In this case, in order to obtain a linear graph, one must plot instead of y,

$$y' = y - \frac{x^2 \left(\int \sigma_{res} \frac{dE}{E}\right)^2_{eff} (E-1)}{1 + x\left(\int \sigma_{res} \frac{dE}{E}\right)_{eff} (E-1)} = y - \Delta \ . \qquad \ldots(12a)$$

This formula is exact according to Equations (1) through (8), but the term Δ involves $\left(\int \sigma_{res} \frac{dE}{E}\right)_{eff}$, which is not known. In order to estimate this term, the effective resonance integrals which had previously been obtained from Figure 10 were used. The values of Δ so calculated are not small at all, being in the order of 13 percent for SRE 7-in., 4 percent for SRE 12-in., and as high as 167 percent for 7-in. natural uranium lattices. The result of making this correction is shown in Figure 11. It will be seen that the correction makes very little improvement in the fit of the points, although the value for A is somewhat increased, as shown in Table X. Evidently, the excess absorption correction is an unnecessary complication, and since its theoretical basis is now believed to be unsound, it is not included in our final results.

TABLE X

PARAMETERS FROM FIGURES 10 AND 11

Lattice Types	A (barns) using $\mathscr{K}_m = 0.00\ cm^{-1}$	A (barns) using $\mathscr{K}_m = 0.12\ cm^{-1}$
7-rod SRE	4.85	6.26
6-rod SRE	5.49	6.52
4-rod	6.42	7.15
7-rod natural	5.21	7.39
Average	5.49 ± 0.46*	6.83 ± 0.44*

*The error cited is merely the average deviation of the tabulated values for A.

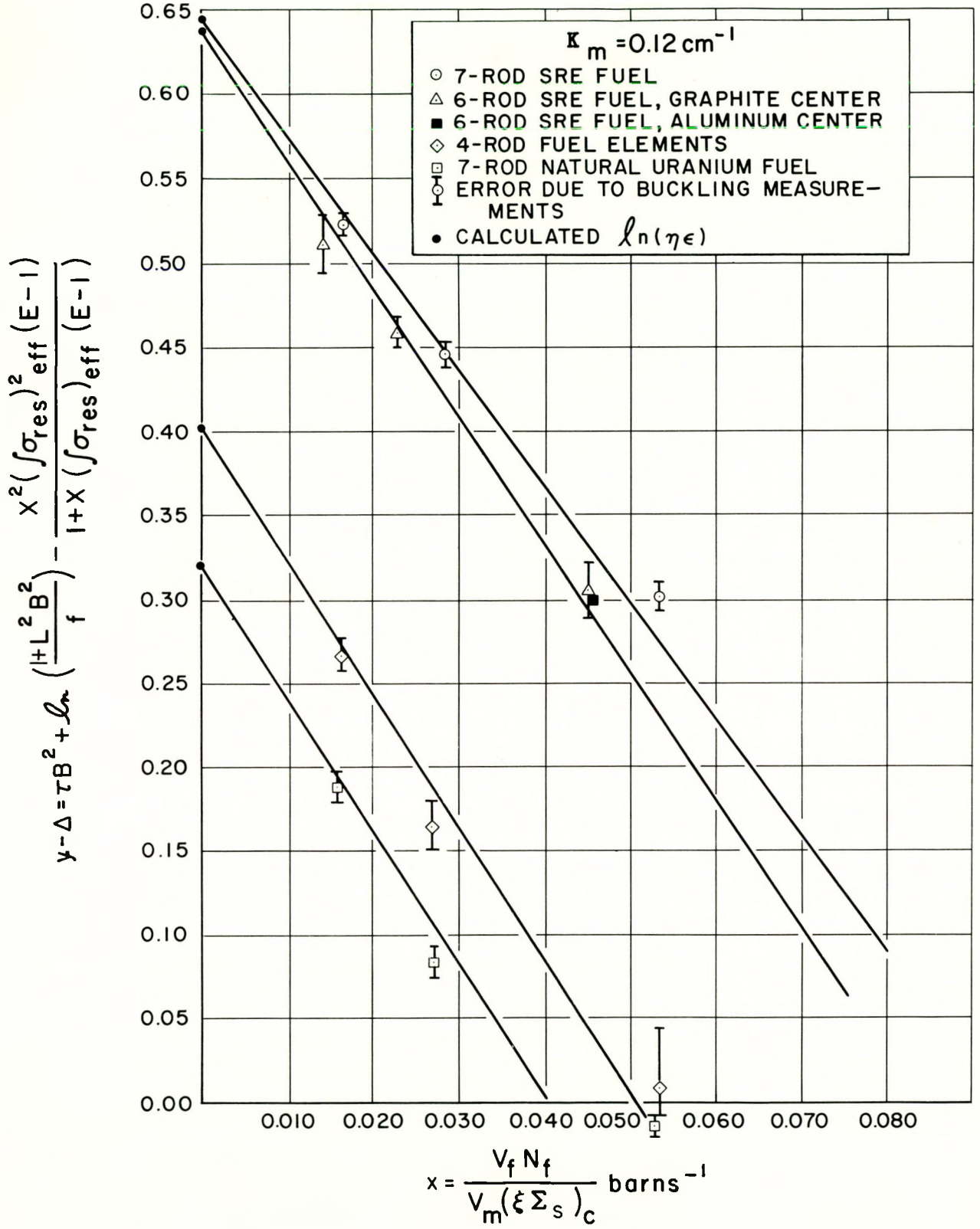

Figure 11. Plot of Equation (12a)

The effect of neutron temperature on these results was next investigated. The previous analysis has assumed the thermal neutron spectrum to be a Maxwellian at room temperature, which is certainly in error. Effects of spectrum hardening due to selective absorption at low energies should be considered. Experimental evidence for this effect may be seen in the cadmium ratio curves shown in Figure 12. A careful evaluation of this correction would be quite complicated, since the flux spectrum is far from Maxwellian in lattices such as these, and in fact may vary markedly even within each material in the cell. In an attempt to evaluate the effect of spectral hardening, an effective neutron temperature was calculated by means of a formula given by E. R. Cohen.[8]

$$T_{eff} = T_0 \left(1 + 0.91\, \overline{m}\, \frac{\overline{\Sigma}_a}{\overline{\Sigma}_s} \right) , \qquad \ldots(13)$$

where the cross sections are cell averaged and taken at 2200 m/sec., and $\overline{m}$ is the atomic weight flux averaged over the cell. The thermal diffusion length is then modified by the formula.

$$L_T^2 = L^2 \sqrt{T_{eff} T_0} \quad .$$

In this investigation, no temperature correction was applied to the thermal utilization, f, because the correction is actually on $(1 - f)$, which is small compared with f. Since the correction is necessarily small in $(1 - f)$, the consequent correction in f will be negligible. When the correction to L^2 is made, it is found that no appreciable improvement in the fit is obtained.

It should be noted that this formula for the effective temperature was not meant to apply to lattice cells, and that the results obtained here in using the formula must be considered merely as indications of the true behavior, and not as quantitatively accurate. There can, however, be no doubt that this spectral hardening exists, and somehow distorts the results. This effect, along with epithermal fission, which was not included in the analysis, will be most important in the 7-in. lattices, where the fuel to moderator ratio is largest. It should also be noted that the 7-in. lattices in this study have a higher fuel to moderator ratio than any lattices for which analyses have been previously reported in the literature.

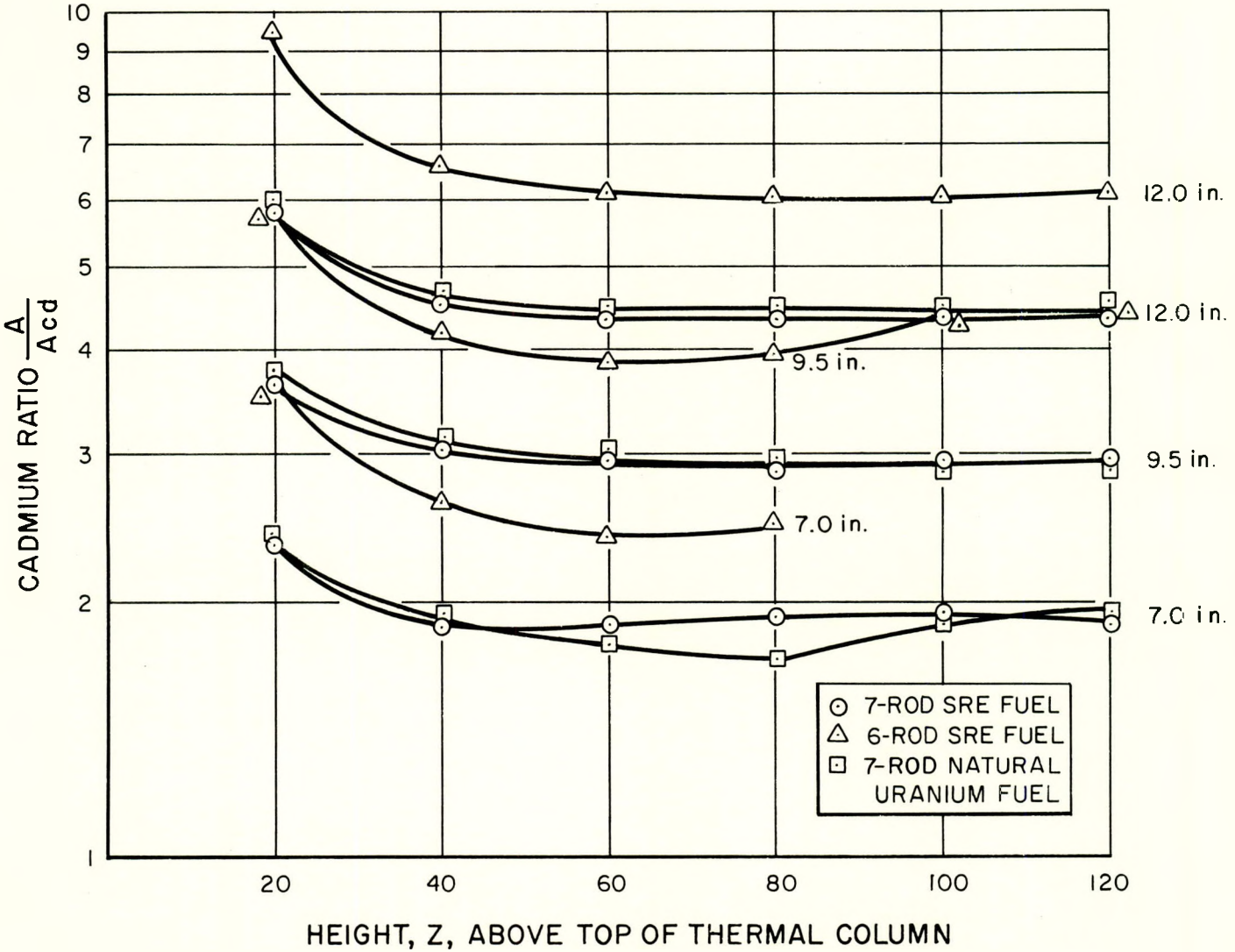

Figure 12. Cadmium Ratios for Several of the Exponential Lattices

The contemplated sodium graphite reactors will have a fuel to moderator ratio approximating the 9.5 in. lattices. Hence, the results obtained by neglecting the 7-in. lattices were considered. One can see from Figure 10 that if the 7-in. lattices are neglected, reasonably straight lines are obtained. The values of A and A' obtained from this calculation, that is, neglecting the 7-in. lattices, are given in Table XI.

The 7-in. lattices always lie above the line drawn in Figure 10. Perhaps this fact is explained by epithermal fission effects, since such a correction would tend to lower these points. It is also in these 7-in. lattices that effects of spectral hardening are most important; so that the calculation of these lattices, neglecting these effects, is necessarily less reliable than in the cases of the 9.5-in. and 12-in. lattices.

TABLE XI

PARAMETERS FROM FIGURES 10 AND 13 NEGLECTING 7-IN. LATTICES

(all values are in barns)

Lattice	From Age Formula Eq (1)			From 2-Group Formula Eq (1a)		
	$\left(\int \sigma_{res} \frac{dE}{E}\right)_{eff}$	A	A'	$\left(\int \sigma_{res} \frac{dE}{E}\right)_{eff}$	A	A'
7-rod SRE	6.25	5.34	0.60	7.83	7.14	2.18
6-rod SRE	6.68	5.49	0.65	8.66	7.71	2.63
4-rod	7.38	6.53	1.56	7.75	6.25	1.93
7-rod natural	7.09	6.48	1.41	7.03	6.75	1.35
Average	6.85 ± 0.36	5.96 ± 0.54	1.055 ± 0.43	7.82 ± 0.43	6.96 ± 0.46	2.02 ± 0.38

The preceding analysis has been made in terms of the age-diffusion relation given in Equation (1). It can also be made in terms of the 2-group relation

$$\eta \epsilon p f = (1 + L^2 B^2)(1 + \tau B^2) \ . \qquad \ldots(1a)$$

Although the age formula is expected to give a better correlation of the experimental results, the value of A derived from it is not the correct one to use in 2-group reactor calculations. In these calculations, one should use a value of A derived from the 2-group formula. Thus, in place of Equation (12), we have

$$ln(\eta\epsilon) - \frac{V_{fuel} N_{fuel}}{V_m (\xi \Sigma_s)_{graphite}}$$

$$ln \frac{(1 + L^2B^2)(1 + \tau B^2)}{f} \quad . \qquad ...(14)$$

Figure 13 show the results of this analysis. Again, the 7-in. lattice points lie too high, and the others determine fairly straight lines. In fact, it is evident that the fit of the points for the 7-in. lattices is even poorer than when the age formula is used. The values of A derived from this graph, neglecting the 7-in. lattices, are given in Table XI. It should be noted that little weight has been given to the 9.5-in. natural uranium lattice, because there is some doubt as to the accuracy of its data.*

The Mummery type analysis yields an average value of the effective resonance integral for a given fuel cluster. Since we are using a calculated value for eta, it is also possible to calculate the value of $\left(\int \sigma_{res} \frac{dE}{E}\right)_{eff}$ for each individual lattice. The values of A obtained in this way are given in Table XII for two values of $\mathcal{K}_m$, and for both the 2-group and the age formulas.

*Flux measurements were taken along a diagonal of the unit cell, and also along a line perpendicular to one face. The thermal flux along the perpendicular must be below those points along the diagonal by an amount which increases with decreasing lattice spacing. This was found to be the case for every lattice where the data were available, except with the 9.5 in., 7-rod natural uranium lattice. This fact indicates that the measurements on this lattice should be viewed with suspicion, or disregarded.

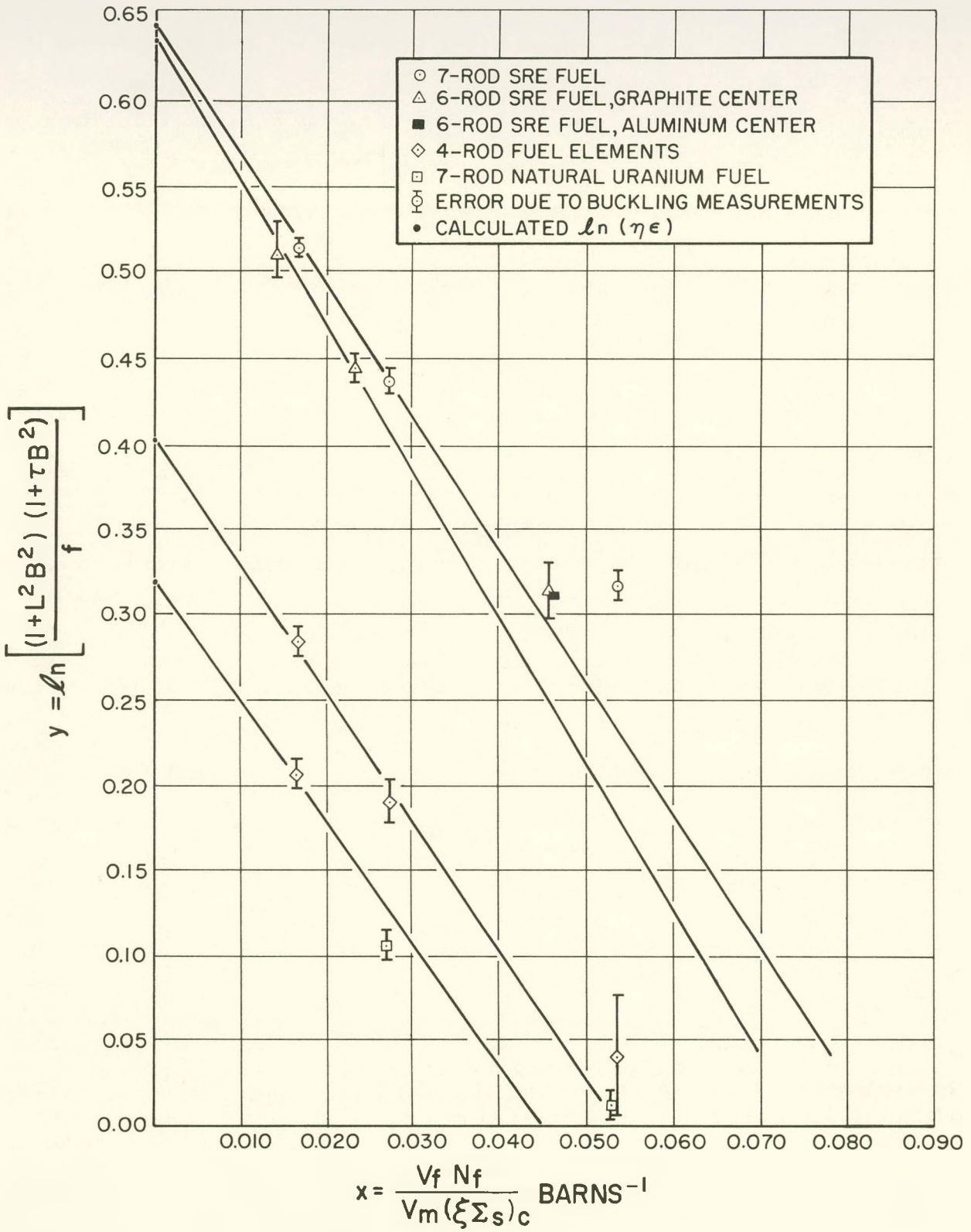

Figure 13. Plot of Equation (13)

TABLE XII

VALUES OF "A" FOR INDIVIDUAL LATTICES

Lattice Spacing (in.)		$\mathscr{B}_m = 0.00\ cm^{-1}$		$\mathscr{B}_m = 0.12\ cm^{-1}$	
		A, using the Age Formula (barns)	A, using the 2-Group Formula (barns)	A, using the Age Formula (barns)	A, using the 2-Group Formula (barns)
7.0	7-rod SRE	4.59	5.23	5.25	6.04
9.5	7-rod SRE	5.47	7.05	6.68	8.92
12.0	7-rod SRE	5.26	7.31	6.69	9.84
7.0	6-rod SRE C-center	5.29	6.00	6.03	6.90
9.5	6-rod SRE C-center	5.55	7.41	6.67	9.21
12.0	6-rod SRE C-center	5.83	8.07	7.35	10.73
7.0	6-rod SRE Al-center	5.36	6.05	6.12	6.96
7.0	4-rod	5.83	5.84	6.81	6.82
9.5	4-rod	7.02	7.06	8.94	9.00
12.0	4-rod	6.15	6.31	8.06	8.29
7.0	7-rod natural	4.69	4.72	5.37	5.40
9.5	7-rod natural	7.33	7.34	9.34	9.35
12.0	7-rod natural	6.21	6.22	8.09	8.10

C. CONCLUSIONS

The purpose of the theoretical analysis of these experiments was not only to correlate the measurements on the exponential assemblies, but also to obtain values for the parameters $\mathscr{B}_m$ and A which can be used to increase the reliability of 2-group calculations for sodium graphite reactors. The correlation of the data was best made by means of the age diffusion formula. It is believed that, within the limits of experimental and theoretical uncertainties, the data are consistently interpreted by this method, although the data for some of the 7-in. lattices show a rather large deviation. However, the accuracy with which the parameters

A and $\mathscr{K}_m$ are determined by these experiments leaves much to be desired, especially if the 7-in. lattices are included. These lattices, though, are definitely undermoderated, and lie outside the range of interest for sodium graphite reactor design.

An attempt to improve the correlations by applying an effective neutron temperature correction to L^2 led to no significant improvement. In the interest of simplicity, this correction is omitted in our final results. It is believed, however, that spectral hardening and epithermal fission effects are important, especially in the 7-in. lattices. A more refined theoretical treatment might succeed in improving the correlation of the 7-in. lattices.

It was found that the choice of $\mathscr{K}_m = 0$ was entirely satisfactory, insofar as substitution of other values for this quantity led to no improvement in the correlation of the data. The values obtained for A and A' which appear in the formulas for the effective resonance integral, are substantially lower than values obtained from foil activation measurements as reported in Reference 6. This fact might be due to the neglect of epithermal fission in this analysis. In Table XIII, our recommended values for A and A', for use in 2-group calculations which neglect epithermal fission, are compared to those of Hellstrand.

TABLE XIII

EFFECTIVE RESONANCE INTEGRAL FOR URANIUM*

	A (barns)	A' (barns)
Age Diffusion	6.0	1.1
Two-Group	7.0	2.0
Hellstrand's Values	7.8	2.81

*Equation 9

APPENDIX

MATERIAL VOLUME FRACTIONS IN THE LATTICES

Lattice (in.)	Graphite	Fuel	Aluminum	Void
7.0 } 7-rod SRE	0.86527	0.06341	0.06754	0.00378
9.5 } 7-rod SRE	0.92683	0.03444	0.03668	0.00205
12.0 } 7-rod SRE	0.95417	0.02159	0.02297	0.00127
7.0 } 6-rod SRE C-center	0.87433	0.05436	0.06754	0.00377
9.5 } 6-rod SRE C-center	0.93175	0.02952	0.03668	0.00205
12.0 } 6-rod SRE C-center	0.95725	0.01849	0.02297	0.00129
7.0 } 6-rod SRE Al-center	0.86527	0.05436	0.07657	0.00380
7.0 } 4-rod	0.86527	0.06357	0.06703	0.00413
9.5 } 4-rod	0.92693	0.03448	0.03636	0.00223
12.0 } 4-rod	0.95417	0.02162	0.02280	0.00141
7.0 } 7-rod natural	0.86527	0.06257	0.06754	0.00462
9.5 } 7-rod natural	0.92693	0.03394	0.03663	0.00250
12.0 } 7-rod natural	0.95417	0.02129	0.02297	0.00157

REFERENCES

1. P. W. Mummery, "The Experimental Basis of Lattice Calculations," A/Conf. 8/5 P429, 1955

2. S. Glasstone and M. C. Edlund, The Elements of Nuclear Reactor Theory, D. Van Nostrand Co., Inc., New York, 1952, p 144

3. D. J. Hughes and S. A. Harvey, "Neutron Cross Section," Brookhaven National Laboratories, Upton, New York, BNL 325, 1955

4. "Neutron Cross Sections," Brookhaven National Laboratories, BNL-170

5. E. Richard Cohen, "Nuclear Science and Engineering," 2 (227-245), 1957

6. E. Hellstrand, "Journal of Applied Physics," 28, 1493, 1957

7. D. J. Behrens, "The Effect of Holes in a Reacting Material on the Passage of Neutrons," AERE-T/R 103

8. E. R. Cohen, "A Survey of Neutron Thermalization Theory," A/Conf. 8/5 P611, 1955